Rev. B 2, 665 (1970).

[15]See, e.g., J. G. Slater and G. F. Koster, Phys. Rev. 94, 1498 (1954).

[16]The susceptibility of $GdNi_2$ has been previously reported by J. A. Cannon, J. I. Budnick, M. P. Kawatra, J. A. Mydosh, and S. S. Kalski, Phys. Letters 35A, 247 (1971). These results are qualitatively similar to the present results and, indeed, provided some of the impetus for our choosing $GdNi_2$ for the present study. The results of Cannon *et al.* differ in detail, however, from the present results in that Curie–Weiss behavior was claimed for $\epsilon > 0.1$, whereas it was claimed only for $\epsilon > 2$ in the present study.

[17]In similar study of EuO, Ref. 3, Curie–Weiss behavior was not observed in the same interval of reduced temperature examined in the present study. The well-defined region of Curie–Weiss behavior observed in the present study allowed a straightforward determination of T_c^{MF}, which is a crucial parameter in any high-temperature model.

[18]This differs from the value $\gamma = 1.10$ reported in the study by Cannon *et al.* (see Ref. 11). The smaller value reported by Cannon *et al.* may reflect the effect of inhomogeneity rounding of the transition in their sample. (See Ref. 6).

[19]R. D. Parks, in *Magnetism and Magnetic Materials* (AIP, New York, 1972), No. 5, p. 630.

[20]F. C. Zumsteg and R. D. Parks, J. Phys. (Paris) 32, 534 (1971).

[21]The most dramatic success of a Landau approach has been in the recent renormalization group work by Wilson and Fisher [K. G. Wilson and M. E. Fisher, Phys. Rev. Letters 28, 240 (1972); K. G. Wilson, *ibid.* 28, 548 (1972)].

PHYSICAL REVIEW B VOLUME 7, NUMBER 1 1 JANUARY 1973

Neutron Scattering Investigation of the Magnetic Excitations in Iron*

H. A. Mook and R. M. Nicklow
Solid State Division, Oak Ridge National Laboratory, Oak Ridge, Tennessee 37830
(Received 21 August 1972)

The spin-wave spectrum of iron has been measured by neutron inelastic scattering using the triple-axis technique. A large crystal of ^{54}Fe (4-at.% Si) was used in most of the measurements to avoid nonmagnetic scattering processes, although a small amount of data was obtained on pure iron. The spin-wave dispersion curves rise nearly quadratically according to the relation $E = Dq^2$, where D was found to be about 260 meV Å^2 for Fe (4-at.% Si) and 280 meV Å^2 for pure iron. The spin-wave intensity was found to decrease slowly with increasing energy until about 85 meV and then to drop rapidly by an order of magnitude. This sudden decrease in the spin-wave intensity is interpreted as resulting from the intersection of the spin-wave dispersion curve with a continuum band of Stoner excitations.

I. INTRODUCTION

Spin-wave measurements on nickel have shown that the spin-wave intensity falls off slowly with increasing energy until about 100 meV, at which point the intensity drops suddenly by an order of magnitude.[1] The intensity dropped off sharply at different energies for the three symmetry directions, disappearing at the lowest energy in the [111] direction and extending out the furthest in the [100] direction. It was assumed that the sudden decrease in intensity was a result of the spin wave intersecting a continuum band of Stoner excitations. We wished to see if similar effects were present in iron, and thus the spin-wave spectra of iron have been measured with care taken to obtain accurate spin-wave intensity data.

The measurements were performed on a triple-axis spectrometer at the High Flux Isotope Reactor (HFIR). Most of the measurements were made on a crystal of ^{54}Fe (4-at.% Si) 1 in. in diameter by 2 in. long. The silicon was added because unwanted crystalline phases prohibited the growth of a large crystal of pure iron. The ^{54}Fe isotope greatly reduced nonmagnetic–inelastic-scattering events. Also, since ^{54}Fe and Si have the same nuclear scattering lengths, incoherent scattering was avoided. The isotope thus gave a much better peak-to-background ratio than could be obtained with a crystal of iron with the normal isotopic composition. Nevertheless, some data were taken with a small crystal of standard Armco iron, although accurate spin-wave-intensity measurements were impossible.

II. SPIN-WAVE SPECTRA

The spin-wave dispersion curves for ^{54}Fe(Si) are shown in Fig. 1. The spin-wave spectra are almost quadratic and appear to be isotropic for the three symmetry directions. The spin-wave spectrum in the [110] direction for Armco iron is shown in Fig. 2. Since the data were hard to obtain for the Armco iron, measurements were made in only one direction. We notice that the spin-wave dispersion relation rises more rapidly for Armco iron than for the Fe (4-at.% Si).

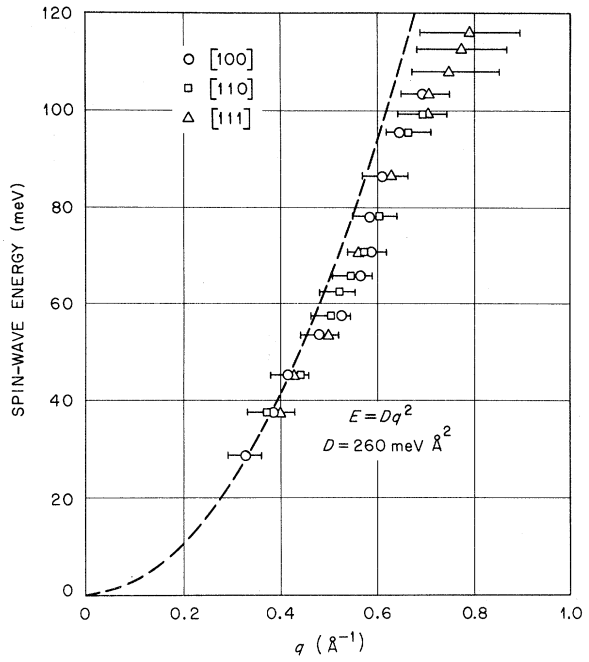

FIG. 1. Spin-wave spectra for Fe (4-at. % Si). The curve shows the relation $E = Dq^2$ for $D = 260$ meV Å^2.

If the spin-wave spectra are described with the relation

$$E = Dq^2(1 - \beta q^2)\,, \qquad (1)$$

it is found by least-squares analysis that D is about 280 meV Å^2 and β is about 0.26 Å^2 for Armco iron. For Fe (4-at.% Si) similar analysis led to values of 260 meV Å^2 and 0.47 Å^2 for D and β, respectively. The quadratic relation alone is plotted in Figs. 1 and 2, and it is easily seen that the spin-wave measurements fall slightly below the quadratic law. The lower-energy part of the dispersion law has previously been measured by Shirane *et al.*[2] They obtained similar values for the quadratic term in Eq. (1) but somewhat larger values for the fourth-order term. However, the uncertainty in the value of the fourth-order term is large, on the order of 50%, and the two measurements were centered about different values of q. In general, the agreement between the two sets of measurements is very good. Most of our results are concentrated at higher energies, where the effects of single-particle excitations on the spin-wave spectrum may be examined.

III. MEASUREMENTS OF SPIN-WAVE INTENSITIES

Since the measurement of spin-wave intensities plays an important role in our results, it is worth considering in some detail how the intensity measurements were made and how the data were processed. The measurements were made on the triple-axis spectrometer shown schematically in Fig. 3. The spin-wave dispersion curve is so steep that constant-momentum-transfer scans are impossible and thus constant-energy-transfer scans were used instead. The spin-wave peaks were thus observed by setting a fixed incoming energy E_0 and a fixed outgoing energy E' by means of the monochromator angle $2\theta_M$ and the analyzer angle $2\theta_A$. The momentum transfer $\overline{K}$ is then determined by the crystal angle ψ and the scattering angle ϕ. The scans were performed by keeping the energy transfer $E_0 - E'$ held constant and varying $\overline{K}$ by stepping the angles ψ and ϕ in such a way that the resolution ellipse of the spectrometer was passed through a dispersion surface along a desired symmetry direction. A spin-wave excitation can thus be measured for a given energy in any desired direction.

The monochromator and analyzer crystals used were beryllium. The (002) reflection was used for the analyzer and the (101) was generally used for the monochromator. Multiple reflections in the monochromator caused dips in the neutron intensity incident upon the sample at certain wavelengths, and it was found that these were minimized if the

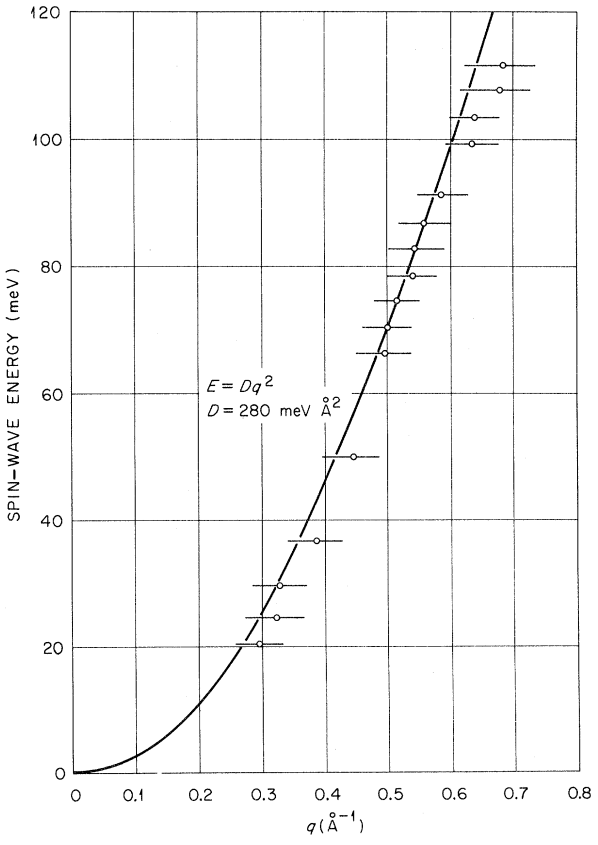

FIG. 2. Spin-wave spectrum for the [110] direction in Armco iron. The curve shows the relation $E = Dq^2$ with $D = 280$ meV Å^2.

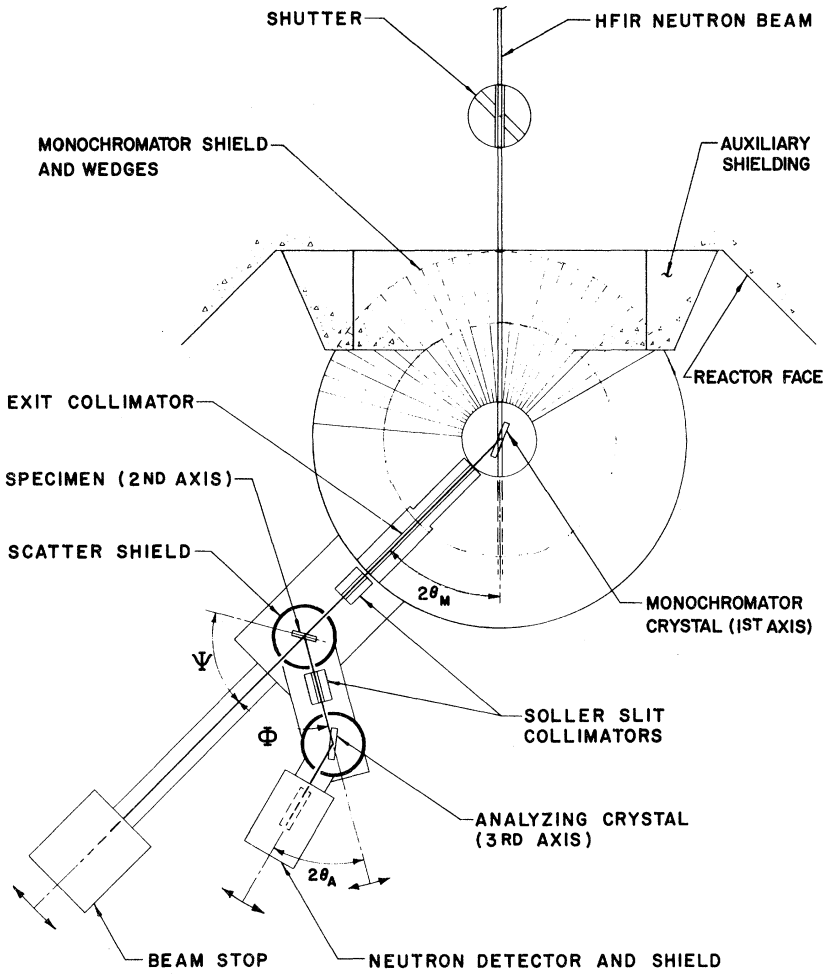

FIG. 3. Schematic diagram of the triple-axis spectrometer at the HFIR.

(101) reflection was used. However, some measurements were checked with both monochromator reflections to make certain that our results were consistent. A monitor counter was used in the monochromatized beam to account for any variations in the incident intensity. However, since counting times were long, we tried to avoid wavelengths that resulted in a loss in intensity from the monochromator because of multiple reflections. In general, $\frac{2}{3}$-deg Soller-slit collimators were used before and after the sample. Some higher-resolution measurements were made with $\frac{1}{3}$-deg horizontal collimation; however, the wider collimation was needed to measure the high-energy low-intensity spin waves. The beam tube limits the angular divergence before the monochromator to about 1°, and no additional collimation was used at that point. Geometrical considerations limit the beam divergence between the analyzer and detector to about 2°, and no additional collimation was used in this position. Since the analyzer angle $2\theta_A$ was held constant during the experiment, extra shielding could be placed around the analyzer position to reduce the background as low as possible.

Brockhouse *et al.*[3] discussed the measurement of phonon intensities with a triple-axis spectrometer. They showed how the interpretation of intensity measurements was greatly simplified if the analyzer angle $2\theta_A$ was held fixed and a monitor counter was utilized to determine the number of neutrons incident upon the sample. However, most of their discussion was centered on the constant-momentum-transfer technique of obtaining data, and we found this technique unsuitable for the steep dispersion curves in iron. Evaluating integrated intensities measured with the constant-energy-transfer technique is not as straightforward as with the constant-momentum-transfer technique, since the Jacobian discussed by Brockhouse *et al.*[3] is not unity for the constant-energy case. The constant-energy case requires some detailed consideration of the resolution of the triple-axis spectrometer.

In recent years resolution of triple-axis spectrometers has been discussed by several authors.[4–8]

The principal conclusion of these studies is that the intensity I observed, when the spectrometer is set for the momentum transfer Q and the energy transfer $\hbar\omega$, is given by the convolution of the scattering cross section $\sigma(Q, \omega)$ with the resolution function of the spectrometer R centered on (Q, ω), viz.,

$$I(\vec{Q}, \omega) = \int R(\vec{Q}+\Delta\vec{Q}, \omega+\Delta\omega)\sigma(\vec{Q}+\Delta\vec{Q}, \omega+\Delta\omega) \times d^3(\Delta\vec{Q})d(\Delta\omega) . \quad (2)$$

The resolution can, to a very good approximation, be described by a Gaussian function in four dimensions as[4]

$$R(\vec{Q}+\Delta\vec{Q}, \omega+\Delta\omega) = R_0 \exp\left(-\frac{1}{2}\sum_{kl} M_{kl}X_kX_l\right), \quad (3)$$

where $X_1 = \Delta Q_x$, $X_2 = \Delta Q_y$, $X_3 = \Delta Q_z$, and $X_4 = \Delta\omega$. R_0 and M_{kl} are involved functions of the mosaic spreads and d spacings of the monochromator and analyzer crystals, the angular divergence of the neutron beam, the wave vectors $\vec{k}_0$ and $\vec{k}'$ of the incident and scattered beam, etc.[4-7] Tucciarone *et al.*[7] have obtained an expression for the total intensity D_0 observed at the spectrometer setting (Q, ω) for the special case of a scattering cross section which is unity. Then, as these authors suggest, one can write R_0 in terms of D_0 as

$$R_0 = D_0/\Delta V , \quad (4)$$

with $\Delta V = \int \exp(-\frac{1}{2}M_{kl}X_kX_l)d^4X$. The expression for D_0 can be written as a product of two functions: one, $D_i(k_0, \theta_M, \alpha_i, \beta_i, \eta_M)$, which describes the intensity of the beam incident on the sample in terms of $\vec{k}_0$, the monochromator mosaic spread η_M, the scattering angle θ_M, and the horizontal and vertical divergences α_i, β_i of the collimators through which this beam passes; the other a similar function $D_f(\vec{k}', \theta_A, \alpha_f, \beta_f, \eta_A)$ which describes the influence of the spectrometer on the intensity of the beam scattered by the sample.

In the present experiment the neutron counts obtained at the detector were normalized by the counting rate $N(k_0)$ of the monitor counter placed in the incident beam just before the sample. In terms of the notation used above

$$N(k_0) = D_i(k_0, \theta_M, \alpha_i, \beta_i, \eta_M)\rho(k_0) , \quad (5)$$

where $\rho(k_0)$ describes the variation with k_0 of the counting efficiency of the monitor.

For spin-wave creation the neutron scattering cross section of the sample can be expressed as

$$\sigma(\vec{Q}, \omega) = (k'/k_0)[S(\vec{Q}, \omega_Q)\delta(\omega-\omega_Q)] , \quad (6)$$

where $S(\vec{Q}, \omega_Q)$ describes the variation of the magnitude of this cross section with $\vec{Q}$, and $\delta(\omega-\omega_Q)$ indicates that for spin waves with infinite lifetime the scattering occurs only on the dispersion surface ω_Q. Thus the neutron intensity obtained at the detector per monitor count is given by

$$\frac{I(\vec{Q}, \omega)}{N(k_0)} = \frac{k}{\Delta V}\int S(\vec{Q}+\Delta\vec{Q}, \omega_{Q+\Delta Q})\delta(\omega+X_4-\omega_{Q+\Delta Q}) \times \exp\left(-\frac{1}{2}\sum_{kl} M_{kl}X_kX_l\right)dX_1dX_2dX_3dX_4 , \quad (7)$$

where $k = D_f(k', \theta_A, \alpha_f, \beta_f, \eta_A)k'/\rho(k_0)k_0$ is a constant, which in the present experiment does not vary from point to point in a given scan or from scan to scan, since $\rho(k_0) \propto k_0^{-1}$, and k' and θ_A were held fixed in all the measurements used to obtain the spin-wave intensities. The effect of occasional changes of k' could be taken into account easily by repeating the same scan for different values of k'.

The integrations indicated in Eq. (7) can of course be carried out numerically. However, before discussing the results of our own numerical calculation, it is perhaps instructive to describe the results that can be obtained in closed form analytically under certain simplifying assumptions. If the variation of $S(\vec{Q}, \omega_Q)$ within the resolution function can be ignored, and if the dispersion surface ω_Q is planar, then Cooper and Nathans[4] have shown that the intensity can be expressed in terms of a function $I(W)$ where

$$I(W) = 2\pi R_{33}(G_1G_2)^{1/2}e^{-G_3^2W^2/2} . \quad (8)$$

Here

$$W = \Delta\omega + \vec{c}\cdot\Delta\vec{Q} ,$$

with $\Delta\omega$ and $\Delta\vec{Q}$ representing the displacement of the midpoint of the resolution function with respect to the point of intersection of the scan and the dispersion plane and $\vec{c}$ being the slope of the dispersion plane. R_{33} represents the integration over the variable X_3, and G_1, G_2, and G_3 are complicated functions of $\vec{c}$ and the M_{kl}. Equation (7) then becomes

$$\frac{I(\vec{Q}, W)}{N(k_0)} = \frac{kS(\vec{Q}, \omega)I(W)}{\Delta V} . \quad (9)$$

The integrated intensity is given by integrating over the variable W. The result we obtain is

$$\int_{-\infty}^{\infty} I(W)dW = \frac{(2\pi)^2(G_1G_2)^{1/2}}{M_{33}G_3} = \Delta V . \quad (10)$$

Although G_1, G_2, and G_3 each depend on $\vec{c}$, the combination $G_3^{-1}(G_1G_2)^{1/2}$ is independent of $\vec{c}$ and varies with M_{kl} in exactly the same way as ΔV. Thus, under the assumptions described above, the integrated intensity of a scan is just $kS(\vec{Q}, \omega)$.

A detailed discussion of the dependence of the observed integrated intensity on the scanning mode is given by Sears and Dolling.[8] For a constant-energy scan with $\vec{c}$ parallel to $\Delta\vec{Q}$, $W = c\Delta Q$. Since it is customary to plot the observed intensity as a

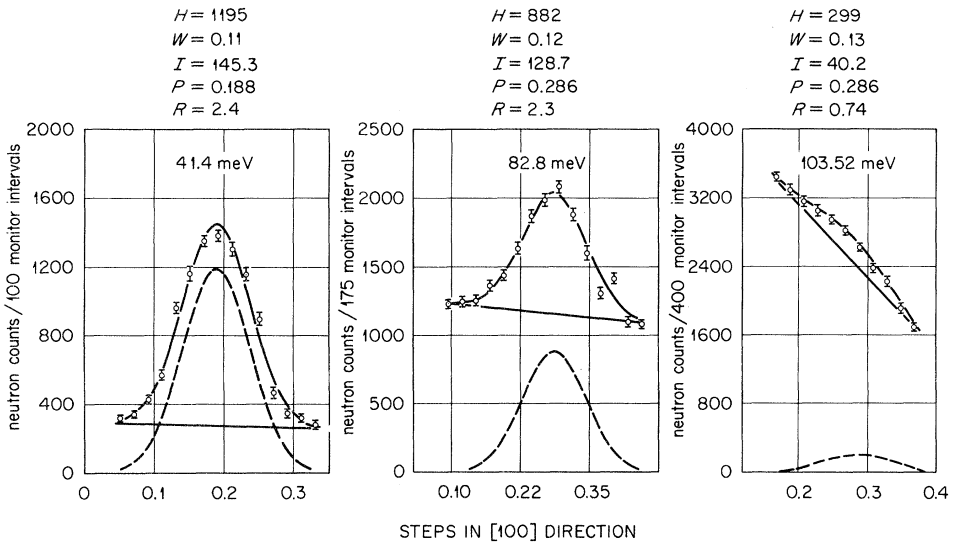

FIG. 4. Spin-wave measurements in the [100] direction for Fe(4-at.% Si) and least-squares computer fits to the data. The dashed curve shows the result of fitting a Gaussian to the measured data and subtracting the background. Parameters shown for the computed Gaussian are the height H, the width W, the integrated intensity I, the peak position P, and the quality-of-fit parameter R.

function of ΔQ , as was done in this experiment, the integration variable is ΔQ and not W. We therefore expect that the integrated intensities obtained in the present work should depend on the reciprocal of the slope of the dispersion surface because

$$\int_{-\infty}^{\infty} I(c\Delta Q)\Delta Q = \frac{1}{c}\int_{-\infty}^{\infty} I(W)dW = \frac{\Delta V}{c} \quad . \tag{11}$$

However, for the relaxed resolution used in this experiment the magnon dispersion surface is not planar within the resolution function. In addition, since the dispersion relation is very nearly a quadratic function of the wave vector, the slope c varies from point to point within the resolution function. In order to investigate the influence of these factors on the integrated intensities obtained with scans at constant energy, we have included them in rather extensive numerical calculations based on Eq. (7), with the assumption that the dispersion surface is a δ function. We have also allowed for the obvious variation of $S(\vec{Q}, \omega)$ within the resolution function due to the magnetic form factor and Boltzmann factor. These calculations show that, within an error of about 10%, the integrated intensities obtained in the present work should also vary as the reciprocal of the dispersion-curve slope, with the slope for each scan evaluated at a magnon energy equal to the energy midpoint of the resolution function. Because this slope varies approximately as the square root of E, it is necessary to adjust the observed intensities by the factor $\sqrt{E}$ before they are compared. The Jacobian in our case is thus assumed to be the factor $\sqrt{E}$, and it must be remembered that our analysis of the spin-wave intensities is based upon the assumption of a quadratic dispersion curve. Of course, the curves deviate slightly from the quadratic law; however, neglect of this fact introduces only a small error in the analysis of the spin-wave-intensity data.

IV. RESULTS

The measured intensities were determined by least-squares fitting of the measured spin-wave peaks with a Gaussian distribution on a sloping background. Since the dispersion surface is not flat the measured peaks are not Gaussian; however, the deviation from Gaussian form is small enough to be neglected. A number R determining the quality of fit to the data was calculated for each spin-wave least-squares fit. R was small in each case, usually less than 3, showing that the Gaussian plus a sloping background gives a satisfactory representation of the data. Spin-wave peaks in the [100] and [111] directions are shown in Figs. 4 and 5. Parameters shown for each peak are the height H, the width W, the peak position P, the integrated intensity I, and the quality-of-fit parameter R. The steps in q are such that the zone boundary is at unity.

Figure 6 shows a comparison between spin waves calculated with numerical techniques based on Eq. (7) and measured spin waves for the [111] direction. To make this comparison the peak height of each calculated scan has been scaled to reproduce the

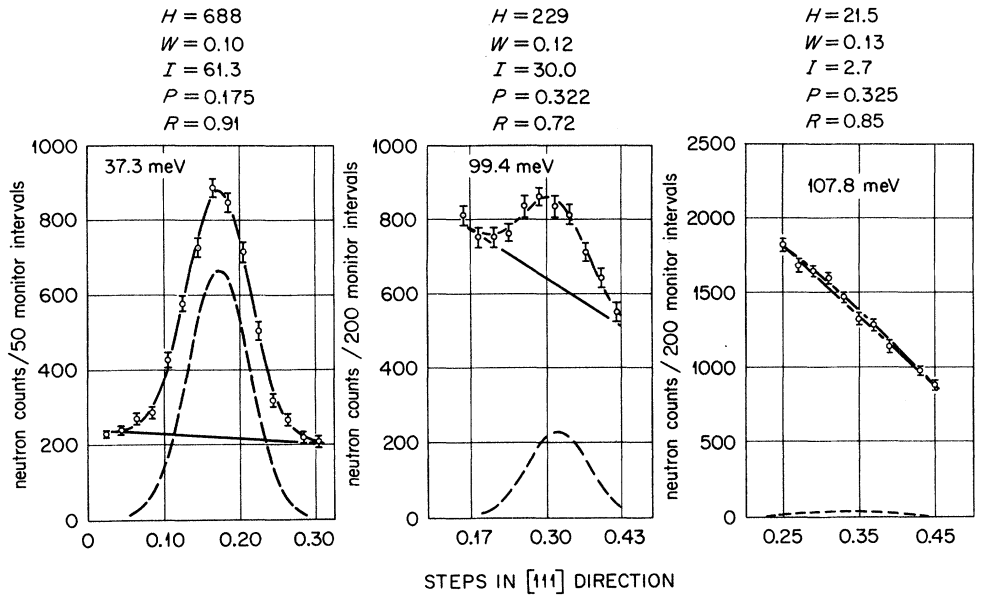

FIG. 5. Spin-wave measurements in the [111] direction for Fe(4-at.%Si) and least-squares computer fits to the data. Parameters shown have the same meaning as in Fig. 4.

observed peak height. The good agreement obtained in the peak shapes demonstrates that our numerical solution of Eq. (7) gives an accurate picture of the operation of the three-axis spectrometer. It is found that the spin-wave intensities fall off rapidly at high energies, and the third measurement in Fig. 6 shows the calculated intensity expected at 107.8 meV based on the measurement at 37.3 meV, if the spin wave had not decreased sharply in intensity.

The spin-wave intensities were normalized by taking the integrated intensities from the computer fits and dividing by the number of neutrons incident upon the sample as determined from the monitor counter. To get the spin-wave intensities independent of energy or momentum transfer the normalized intensities must then be divided by the square of the magnetic form factor and multiplied by the Boltzmann factor.[9] The form factor for iron has been determined to very good accuracy by Shull and Yamada[10] and the Boltzmann factor is easily found from the parameters of the measurement. This result must then be corrected with the $\sqrt{E}$ Jacobian factor.

The final corrected intensities normalized to unity at zero energy transfer are plotted in Fig. 7 as a function of energy. We note that the spin-wave intensity falls off slowly with increasing energy until about 80 meV, at which time the intensity decreases rapidly by an order of magnitude. We assume that this sudden decrease is caused by the

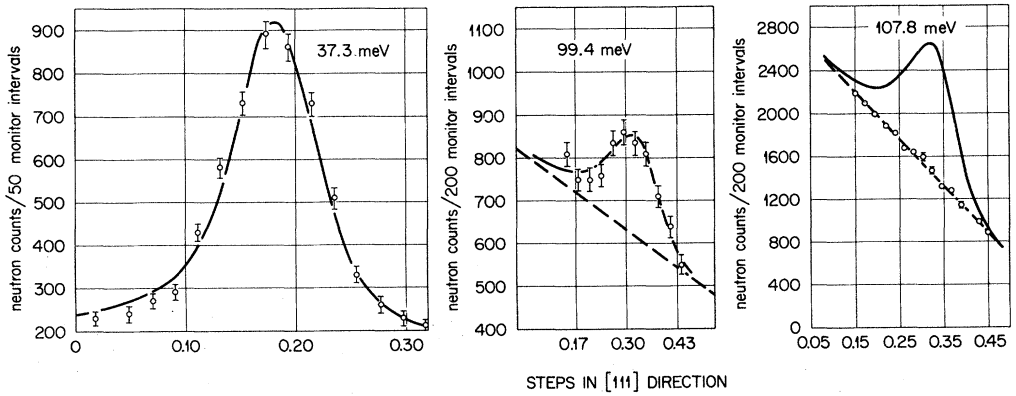

FIG. 6. Comparison of calculated and measured spin-wave excitations. The third graph shows the peak expected if the spin-wave cross section remained a constant independent of energy.

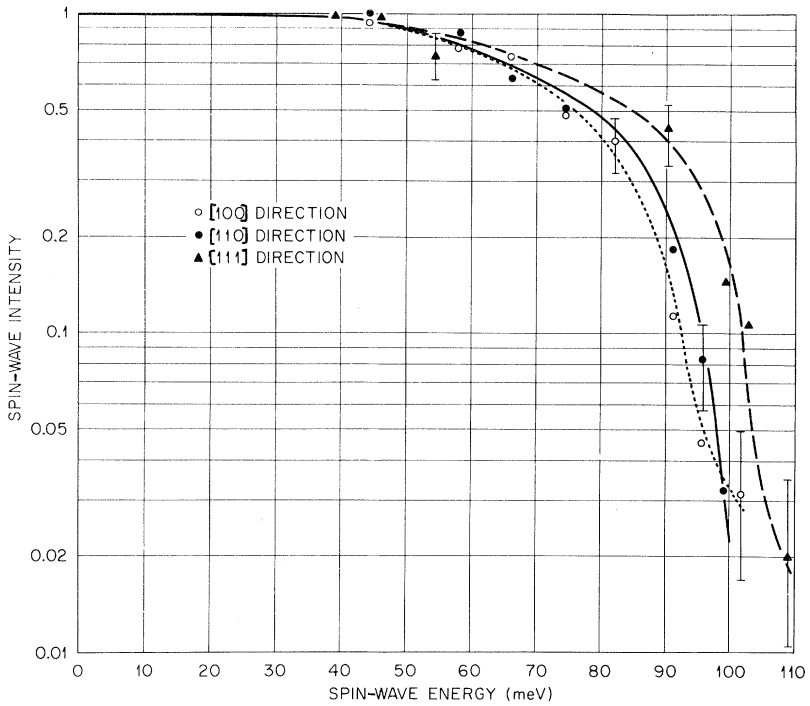

FIG. 7. Spin-wave intensity as a function of energy for Fe (4-at.% Si).

intersection of the spin-wave spectra with a continuum band of Stoner excitations. The intersection point appears to be slightly different for the three symmetry directions, being highest in the [111] direction and lowest in the [100] direction. Neutron scattering from the Stoner excitations is not expected to be observable since the single-particle excitations are very broad in energy. Only a very small amount of scattering from them falls within the resolution function of the spectrometer, and this is indistinguishable from the room background. The intersection point of the spin waves with the Stoner excitations agrees fairly well with calculations by Thompson and Mook[11] from the energy bands for iron.

The experiment is difficult because very-small-intensity spin waves must be measured to determine the position of the Stoner continuum. We notice from Fig. 5 that for the lowest-energy spin-wave peaks there are about 700 counts in the peak in 50 monitor intervals, which corresponds to about 5 min counting time per point. At the high incident energies needed to measure the high-energy spin waves the reactor flux is greatly reduced and the number of monitor counts used was increased to about 400, making counting times very long. However, this is the only type of experiment that can give a direct measurement of the influence of the Stoner single-particle excitations on the spin-wave dispersion relations.

---

*Research sponsored by the U. S. Atomic Energy Commission under contract with Union Carbide Corporation.

[1]H. A. Mook, R. M. Nicklow, E. D. Thompson, and M. K. Wilkinson, J. Appl. Phys. 40, 1450 (1969).

[2]G. Shirane, V. J. Minkiewicz, and R. Nathans, J. Appl. Phys. 39, 383 (1968).

[3]B. N. Brockhouse, L. N. Becka, K. P. Rao, and A. D. B. Woods, in *Second Symposium on Inelastic Scattering of Neutrons in Solids and Liquids* (International Atomic Energy Agency, Vienna, 1963), Vol. II, p. 23.

[4]M. J. Cooper and R. Nathans, Acta Cryst. 23, 357 (1967).

[5]H. Bjerrum Møller and M. Nielsen, *Instrumentation for Neutron Inelastic Scattering Research* (International Atomic Energy Agency, Vienna, 1970), p. 49.

[6]S. A. Werner and R. Pynn, J. Appl. Phys. 42, 4736 (1971).

[7]A. Tucciarone, H. Y. Lau, L. M. Corliss, A. Delapalme, and J. M. Hastings, Phys. Rev. B 4, 3206 (1971).

[8]V. F. Sears and G. Dolling, AEC Report No. 4133, 1972 (unpublished).

[9]The cross section for spin-wave scattering is discussed by a number of authors. See for instance, T. Izuyama, D. Kim, and R. Kubo, J. Phys. Soc. Japan 18, 1026 (1963); or W. Marshall and S. W. Lovesey, *Theory of Thermal Neutron Scattering* (Oxford U. P., Oxford, England, 1971).

[10]C. G. Shull and Y. Yamada, J. Phys. Soc. Japan Suppl. 17 B-III, 1 (1962).

[11]E. D. Thompson and H. A. Mook, J. Appl. Phys. 41, 1227 (1970).